J|A|C|S
ARTICLES
Published on Web 03/06/2004

Molecular View of the Anomalous Acidities of Sn^{2+}, Pb^{2+}, and Hg^{2+}

Hazel Cox* and Anthony J. Stace*

Contribution from the School of Chemistry, Physics and Environmental Science, University of Sussex, Falmer, Brighton BN1 9QJ, United Kingdom

Received October 27, 2003; E-mail: a.j.stace@sussex.ac.uk

Abstract: Experimental results taken from both the condensed and gaseous phase show that, when associated with water, the three dications Sn^{2+}, Pb^{2+}, and Hg^{2+} exhibit a facile proton-transfer reaction. In the gas phase, no stable $[M\cdot(H_2O)_n]^{2+}$ ions are observed; but instead the cations appear to undergo rapid hydrolysis to give ions of the form $M^+OH(H_2O)_{n-1}$. A series of ab initio calculations have been undertaken on the structures and proton-transfer reaction profiles associated with the complexes $[M\cdot(H_2O)_{2,4}]^{2+}$, where M is one of Sn, Pb, Hg, and Ca. The latter has been used as a reference point both in terms of comparisons with previous calculations, and the fact that Ca^{2+} is a very weak acid. The calculations show that for Sn^{2+}, Pb^{2+}, and Hg^{2+}, the only barriers to proton transfer are those associated with the movement of water molecules. In the gas phase, these barriers could be overcome through energy gained during ion formation, and in the condensed phase the thermal motion of water molecules would be sufficient. In contrast, the calculations show that for Ca^{2+} it is the proton-transfer step that provides the most significant reaction barrier. Proton transfer in Sn^{2+} and Pb^{2+} is further assisted by distortions in the geometries of $[M\cdot(H_2O)_{2,4}]^{2+}$ complexes due to voids created by the $5s^2$ ($6s^2$) inert lone pair. For Hg^{2+}, ease of proton transfer is derived partly from the high degree of covalent bonding found in both the reactants and products.

1. Introduction

Within inorganic chemistry the hydrolysis reaction as defined by eq 1 is ubiquitous.[1]

$$M^{n+} + 2H_2O \leftrightarrow [M\cdot(H_2O)_2]^{n+} \leftrightarrow M(OH)^{(n-1)+} + H_3O^+ \quad (1)$$

Most metal cations form strong bonds with oxygen and bulk water offers a small but constant supply of reactive OH^- via the autoprotolysis constant, $K_w = [H_3O^+][OH^-] \approx 10^{-14}$. Thus, for all doubly charged metal cations it is possible to define a hydrolysis constant, K_h, as[1]

$$K_h = \frac{[MOH^+][H_3^+O]}{[M^{2+}]} \quad (2)$$

which can be seen as a measure of the aqueous acidic strength of the M^{2+} cation. In many instances a more realistic description of M^+OH is probably $M^{2+}OH^-$, which reflects the ionic nature of the metal−oxygen bond. For a wide range of doubly charged metal ions, there exists a reasonably good correlation between their pK_h ($= -\log K_h$) and their charge-to-size ratio (q^2/r_{ion}).[2,3] pK_h could be viewed as a measure of the work done to remove a proton from a metal ion−water complex to infinity.[2] Similarly, the electrostatic term, q^2/r_{ion}, reflects the contribution Coulomb repulsion between the two separating charges makes to the energetics of proton release. Thus, for a large ion, such as Ba^{2+} ($pK_h \approx 13$) this contribution is negligible, but for Be^{2+} ($pK_h = 5.5$), Coulomb repulsion makes a very significant contribution to the exothermicity of reaction 1. Three metal cations, Sn^{2+}, Pb^{2+}, and Hg^{2+}, stand out quite markedly from the trend that exists between pK_h and q^2/r_{ion}.[3] The implication is that all three appear to be more acidic than would be predicted purely from their size, and that additional factors, apart from the development of a hydration shell, influence the magnitude of pK_h. As an example, Ca^{2+} and Sr^{2+} are comparable in size to Pb^{2+} and yet the latter has a pK_h of ∼8, compared with ∼12 for the other two ions.

The properties that distinguish Sn^{2+}, Pb^{2+}, and Hg^{2+} from most other metal dications, are derived from condensed phase behavior. However, recent experiments on the gas phase solvation of metal dications show a remarkably similar pattern of behavior.[4,5] Apart from Sn^{2+}, Pb^{2+}, and Hg^{2+}, stable $[M\cdot(H_2O)_n]^{2+}$ complexes have been identified in the gas phase for most metal dications using mass spectrometric methods.[6−9] In some cases these complexes are stable with just a single water

(1) Baes, C. F., Jr.; Mesmer, R. E. *The Hydrolysis of Cations*: Wiley J.; New York, 1976.
(2) Shriver, D. F.; Atkins, P. W. *Inorganic Chemistry*: OUP; Oxford, 1999.
(3) Stace, A. J. *J. Phys. Chem. A* **2002**, *106*, 7993.
(4) Cheng, Z. L.; Siu, K. M.; Guevremont, R.; Berman, S. S. *J. Am. Soc. Mass Spectrom.* **1992**, *3*, 281.
(5) Akibo-Bett, G.; Barran, P. E.; Puskar, L.; Duncombe, B.; Cox, H.; Stace, A. J. *J. Am. Chem.. Soc.* **2002**, *124*, 9257.
(6) Jayaweera, P.; Blades, A. T.; Ikonomou, M. G.; Kebarle, P. *J. Am. Chem. Soc.* **1990**, *112*, 2452.
(7) Blades, A. T.; Jayaweera, P.; Ikonomou, M. G.; Kebarle, P. *Int. J. Mass Spectrum. Ion Processes* **1990**, *102*, 251.
(8) Blades, A. T.; Jayaweera, P.; Ikonomou, M. G.; Kebarle, P. *J. Chem. Phys.* **1990**, *92*, 5900.
(9) Stace, A. J.; Walker, N. R.; Firth, S. *J. Am. Chem. Soc.* **1997**, *119*, 10 239.

molecule;[10−12] however most achieve maximum stability (intensity) in the presence of four or more molecules. In the case of Sn^{2+}, Pb^{2+}, and Hg^{2+},[4,5] the ions observed in the gas-phase experiments have the form $MOH^+(H_2O)_n$, i.e., they are the hydrolysis product resulting from reaction 1 going to completion. In effect, the cations behave as very strong acids in the presence of small numbers of water molecules. What is interesting about this observation is that it does not rely on any of the underlying properties of bulk water, such as K_w, because the latter quantity has no meaning in the presence of just a few molecules.[13] Particularly in the case of Pb^{2+}, it could be argued that the presence of a small concentration of H_3O^+ in bulk water serves to moderate the acidity of the metal ion by shifting the equilibrium in eq 1 to the left. The absence of that 'bulk' constraint on the behavior of the gas-phase complex, means that the hydrolysis reaction does not attain equilibrium. Several metal cation system have been shown to exhibit a range of ions in the gas phase; for example, both $[Mg\cdot(H_2O)_n]^{2+}$ and $MgOH^+\cdot(H_2O)_{n-1}$ are observed in the mass spectrum of a typical pickup or electrospray study of magnesium/water complexes.[14] However, the appearance of both hydrolysis reactant and product in the same experiment does not imply an equilibrium, but instead signifies the presence of a substantial activation barrier to proton transfer.

In terms of the anomalous acidities of Sn^{2+}, Pb^{2+}, and Hg^{2+}, the gas phase results also demonstrate that the driving force behind their acidity is not derived solely from effects associated with these ions in bulk water. The results suggest that the high acidities of Sn^{2+}, Pb^{2+}, and Hg^{2+} are precipitated through configurations adopted by small numbers of water molecules when they interact with each of the cations. One possible driving force that could have a more dominant role in the gaseous rather than condensed phase is charge transfer. Many metal ions have second ionization energies ($M^+ \rightarrow M^{2+} + e^-$) that are higher than the first ionization energy of water. Therefore, the most likely outcome from a gas-phase encounter between M^{2+} and a water molecule would be $MOH^+ + H^+$, i.e., products of a hydrolysis reaction.[13] However, the fact that there are techniques which can prepare single-molecule $M^{2+}\cdot H_2O$ complexes in the gas phase, means that there exist states that are either stable or metastable with respect to the large differences in ionization energy.[10−12,15] Since the ionization energy difference between water and any of the three metals is not particularly anomalous, Sn^{2+}, Pb^{2+}, and Hg^{2+} should not be expected to behave very differently from other M^{2+} ions with respect to charge transfer.[16]

Several papers have recently addressed the issue of acidity on the part of metal ions from a theoretical perspective. Glusker, Bock and co-workers have calculated a range of properties associated with $M^{n+}[OH_2]_p$ complexes for $n = 1$ and 2, and for $p = 1$ and 6.[17,18] Their work has shown that factors, such as the metal−oxygen bond length and the enthalpy of hydration of monohydrates correlate quite well with pK_h, and they have concluded that the properties of metal monohydrates reflect many of the characteristics required of the hydrolysis mechanism. Both Chang and Wang,[19] and Glusker and Bock et al.[20] have used theory to demonstrate that there exist linear relationships between pK_h and the properties of both mono- and hexahydrate metal ion complexes. An important conclusion to emerge from this body of work, and one that has significance for the topic addressed here, is that as the degree of hydration of M^{n+} increases, the enthalpy change associated with deprotonation (hydrolysis) decreases. The relative energy difference between $M^{n+} + OH^-$ and $M^{n+} + H_2O$ declines as more water molecules are added to the metal. Neither Chang and Wang[19] nor Glusker and Bock et al.[17,18,20] included tin, lead or mercury in their studies of acidity in metal ions. In a separate theoretical study, Beyer et al.[21] examined the unimolecular decay of $M^{2+}\text{-}(H_2O)_2$ complexes, where M is an alkaline earth metal. By proposing a 'salt bridge' mechanism (see below), they were able to account for some of the observations of Spears et al.[22] and Kebarle and co-workers[6,7,8] on gas-phase experiments involving the same metal cations. Again, none of this work included tin, lead or mercury. Reaction pathways calculated for proton transfer from complexes of water with Zn^{2+}, Be^{2+}, and Mg^{2+} have also been presented by Solà et al.[23]

Our intention here is to use ab initio methods to identify stable structures involving Sn^{2+}, Pb^{2+}, and Hg^{2+} in association with two and four water molecules. We will show that by understanding the nature of the interaction between the metal ions and the solvent molecules, it is possible to account for the underlying instability of each of the corresponding $[M\cdot(H_2O)_n]^{2+}$ complexes. Since Sn^{2+} and Pb^{2+} appear to follow a common pattern, our analysis will examine these two ions together. We shall then consider the acidic behavior of Hg^{2+} separately and, for the purposes of a reference, data on Ca^{2+} will also be presented.

There are two important differences between acidity in the condensed phase and the type of gas phase process referred to here, namely irreversible intercluster proton transfer. First, acidity in the condensed phase will be moderated by the presence of an autoionising solvent. Second, the kinetics of an irreversible process in the gas phase is primarily determined by the magnitude of any activation barrier, and how it compares with internal energy acquired as a result of formation, e.g., electron impact ionization or collisions with a buffer gas. An extreme case would be the complete absence of a barrier, in which case only reaction products would be observed on the time scale of a typical experiment ($\sim 10^{-4}$ s). In contrast, the only important quantity in the condensed phase is the difference in free energy (ΔG) between the reactants and products (as shown in eq 1).[24] Even through Hg^{2+} and Sn^{2+} appear to be very acidic, from the relationship $\Delta G = RT\ pK_h$, it can be seen that their free energy differences are still positive, but quite

(10) Shvartsburg, A. A.; Siu, K. W. M. *J. Am. Chem. Soc.* **2001**, *123*, 10 071.
(11) Stone, J. A.; Vukomanovic, D. *Chem. Phys. Lett.* **2001**, *346*, 419.
(12) Schroder, D.; Schwarz, H.; Jianglin, W.; Wesdemiotis, C. *Chem. Phys. Lett.* **2001**, *343*, 258.
(13) Stace, A. J. *J. Phys. Chem. A* **2002**, *106*, 7993.
(14) Walker, N.; Dobson, M. P.; Wright, R. R.; Barran, P. E.; Murrell, J. N.; Stace, A. J. *J. Am. Chem. Soc.* **2000**, *122*, 11 138.
(15) El-Nahas, A. M.; Tajima, N.; Hirao, K. *Chem. Phys. Lett.* **2000**, *318*, 333.
(16) Soldan, P.; Lee, E. P. F.; Wright, T. G. *J. Phys. Chem. A* **2002**, *106*, 8619.
(17) Trachtman, M.; Markham, G. D.; Glusker, J. P.; George, P.; Bock, C. W. *Inorg. Chem.* **1998**, *37*, 4421.
(18) Trachtman, M.; Markham, G. D.; Glusker, J. P.; George, P.; Bock, C. W. *Inorg. Chem.* **2001**, *40*, 4230.
(19) Chang, C. M.; Wang, M. K. *Chem. Phys. Lett.* **1998**, *286*, 46.
(20) George, P.; Glusker, J. P.; Trachtman, M.; Bock, C. W. *Chem. Phys. Lett.* **2002**, *351*, 454.
(21) Beyer, M.; Williams, E. R.; Bondybey, V. E. *J. Am. Chem. Soc.* **1999**, *121*, 1565.
(22) Spears, K. G.; Fehsenfeld, F. C.; McFarland, M.; Ferguson, E. E. *J. Chem. Phys.* **1972**, *56*, 2562.
(23) Solà, M.; Lledós, A.; Duran, M.; Bertrá, J. *Theor. Chim. Acta* **1992**, *81*, 303.
(24) Atkins, P.; de Paula, J. *Atkins' Physical Chemistry*: OUP; Oxford, 2002.

small; $Sn^{2+} \cong 5$ kJ mol^{-1}; $Hg^{2+} \cong 9$ kJ mol^{-1}. These values are well within the energy range available under thermal conditions.

2. Computational Details

All calculations were performed using the Gaussian 98[25] suite of programs. To facilitate comparisons across the range of metal dications, effective core potentials (ECP) were used with the inclusion of some relativistic effects for the larger nuclei (Sn, Pb, and Hg). Initial calculations were performed using the LANL2DZ basis set, and as a test of suitability the dissociation energy of $[Ca-OH]^+$ was calculated and compared with experiment. Interestingly, this basis set performed extremely well (experimentally derived $D[Ca-OH]^+ = 1403.6$ kJ mol^{-1}, compared with the calculated value of 1374.5 kJ mol^{-1}), and produced an error of approximately 2% for calcium hydroxide. However, if instead of simply subtracting the calculated energies of Ca^{2+} and OH^- from that of the entity $[Ca-OH]^+$, the dissociation energy is calculated using the recipe prescribed by Beyer et al,[21] i.e.

$$D(Ca^{2+}-OH^-) = IE(Ca^+) + D(Ca^+ - OH) - EA(OH) \quad (3)$$

then the agreement of the individual components with experiment is extremely poor. IE is the ionization energy and EA is the electron affinity. In particular, the electron affinity of OH is in error by 96% and even when diffuse functions are added the error is still approximately 19%, which would suggest that the above agreement with experiment is merely fortuitous.

Therefore, all calculations presented in this paper use a metal pseudopotential developed by the Stuttgart/Bonn group (denoted SDD in Gaussian 98) and the standard 6-31+G(d,p) basis set for oxygen and hydrogen. For each metal, there is available a choice of reference data for use in deriving a pseudopotential.[26] In this work, the following effective core potentials (ECPs) were found to be adequate: Ca ECP10MWB (4s 4p 1d)/[2s 2p 1d]; Sn ECP46MWB (4s 4p)/[2s 2p]; Pb ECP78MWB (4s 4p 1d)/[2s 2p 1d]; Hg ECP60MWB (8s 7p 6d)/[6s 5p 3d]. For these ECPs the data were fitted to the neutral atom using the quasi-relativistic formulizm of Wood-Boring (WB) and also included polarization functions.[27−30] This combination of basis functions gave an approximately constant error (<15%) in each of the terms in eq 3 for all the metal hydroxide systems considered in this paper; thus improving the validity of comparisons between metal complexes.

Geometry optimizations and frequency calculations were performed at the MP2 level and the frequencies and zero point energies were scaled by 0.9646. Single point energy calculations were performed using CCSD(T) theory at the MP2 optimized geometry to include electron correlation. For the dihydrate complexes, a 6-311+G (d, p) basis set was used for oxygen and hydrogen (resource limitations prevented a similar treatment for tetra-hydrate complexes). Natural population analysis (NPA) was performed using the MP2 electron density. Transition states were located using the synchronous transit-guided Quasi-Newton (STQN) methods as implemented in Gaussian 98.[25] For systems with two water molecules, the QST2 function was used successfully to generate a guess structure for the transition state (TS) based upon the geometries of reactants and products. For larger systems, it was often necessary to provide a guess structure using the QST3 function. These initial structures were located by performing a potential energy surface scan, whereby a series of geometry optimizations are performed on structures related by an assumed reaction coordinate.

All transition states were examined using an intrinsic reaction coordinate (IRC) calculation,[25] which examines reaction pathways leading down from a transition state. Each calculation starts at the saddle point and follows the path in both directions from a transition state, optimizing the geometry at each point. In this way, an IRC calculation connects two minima on the PES by a path that passes through the TS between them. However, in most cases, it will not step all the way to the minimum either side of the path. Therefore, full geometry optimizations were performed on the last geometric structure in each direction. Although this may appear excessive, experience showed that for the shallow potentials on the tin and lead surfaces (especially with four water molecules), it was necessary to ensure that complete reaction pathways were calculated. In fact, this method proved successful in locating a second intermediate stage in each of the reaction pathways for these two metals, and was, therefore, used routinely for all systems investigated.

3. Results and Discussion

The three dications of interest are all closed shell: Sn^{2+} (s^2), Pb^{2+} (s^2), and Hg^{2+} (d^{10}). Therefore, ligand-field stabilization (LFS) is not a factor in determining the coordination of water molecules. To help distinguish the unusual behavior of these ions in an aqueous environment, comparisons are made with Ca^{2+}, which, being a d^0 system, is also closed-shell and as such is also not influenced by LFS. Furthermore, Ca^{2+} and Hg^{2+} are of similar size (100 and 96 pm, respectively), thus a comparison of their complexes may help to illustrate differences between primarily electrostatic binding and binding that involves a significant degree of charge transfer. In addition, there have been several earlier theoretical studies of the hydration of alkaline earth metal,[21,31−35] and comparisons with the Ca^{2+} results presented here will help to validate our procedures.

(i) Initial Geometries. Figure 1 shows minimum energy structures calculated for $[Sn(H_2O)_2]^{2+}$ and $[Hg(H_2O)_2]^{2+}$. Other results show the geometry of $[Pb(H_2O)_2]^{2+}$ to be very similar to that given for the Sn^{2+} complex, and the calculated structure of $[Ca(H_2O)_2]^{2+}$ to be approximately linear with a bond angle close to 180°. Previous work by a number of groups has shown that the inclusion of d orbitals in the Ca^{2+} basis set leads to $[Ca(H_2O)_2]^{2+}$ having a nonlinear structure, which is attributed to core polarization.[31−33,36] Kaupp and co-workers reached a similar conclusion regarding CaF_2, where calculations showed that d-orbital participation contributed to the molecule forming a bent structure.[37] However, in all of these studies, the bending potentials have very shallow barriers, which are negligible when compared with the internal energy an ion might have in a typical

(25) Frisch, M. J.; Trucks, G. W.; Schlegel, H. B.; Scuseria, G. E.; Robb, M. A.; Cheeseman, J. R.; Zakrzewski, V. G.; Montgomery, J. A.; Stratmann, R. E.; Burant, J. C.; Dapprich, S.; Millam, J. M.; Daniels, A. D.; Kudin, K. N.; Strain, M. C.; Farkas, O.; Tomasi, J.; Barone, V.; Cossi, M.; Cammi, R.; Mennucci, B.; Pomelli, C.; Adamo, C.; Clifford, S.; Ochterski, J.; Petersson, G. A.; Ayala, P. Y.; Cui, Q.; Morokuma, K.; Malick, D. K.; Rabuck, A. D.; Raghavachari, K.; Foresman, J. B.; Cioslowski, J.; Ortiz, J. V.; Stefanov, B. B.; Liu, G.; Liashenko, A.; Piskorz, P.; Komaromi, I.; Gomperts, R.; Martin, R. L.; Fox, D. J.; Keith, T.; Al-Laham, M. A.; Peng, C. Y.; Nanayakkara, A.; Gonzalez, C.; Challacombe, M.; Gill, P. M. W.; Johnson, B. G.; Chen, W.; Wong, M. W.; Andres, J. L.; Head-Gordon, M.; Replogle, E. S.; Pople, J. A. *Gaussian 98*, Revision A.7, Gaussian, Inc., Pittsburgh, PA, 1998.

(26) http://www.theochem.uni-stuttgart.de.
(27) Andrae, D.; Haeussermann, U.; Dolg, M.; Stoll, H.; Preuss, H. *Theor. Chim. Acta* **1990**, *77*, 123.
(28) Kuechle, W.; Dolg, M.; Stoll, H.; Preuss, H. *Mol. Phys.* **1991**, *74*, 1245.
(29) Kaupp, M.; Schleyer, P. v. R.; Stoll, H.; Preuss, H. *J. Chem. Phys.* **1991**, *94*, 1360.
(30) Bergner, A.; Dolg, M.; Kuechle, W.; Stoll, H.; Preuss, H. *Mol. Phys.* **1993**, *80*, 1431.
(31) Bauschlicher, C. W.; Sodupe, M.; Partridge, H. *J. Chem. Phys.* **1992**, *96*, 4453.
(32) Glendening, E. D.; Feller, D. *J. Phys. Chem.* **1996**, *100*, 4790.
(33) Katz, A. K.; Glusker, J. P.; Beebe, S. A.; Bock, C. W. *J. Am. Chem. Soc.* **1996**, *118*, 5752.
(34) Pavlov, M.; Siegbahn, P. M. E.; Sandström *J. Phys. Chem. A* **1998**, *102*, 219.
(35) Peschke, M.; Blades, A. T.; Kebarle, P. *J. Phys. Chem. A* **1998**, *102*, 9978.
(36) Kaupp, M.; Schleyer, P. v. R. *J. Phys. Chem.* **1992**, *96*, 7316.
(37) Kaupp, M.; Schleyer, P. v. R.; Stoll, H.; Preuss, H. *J. Am. Chem. Soc.* **1991**, *113*, 6012.

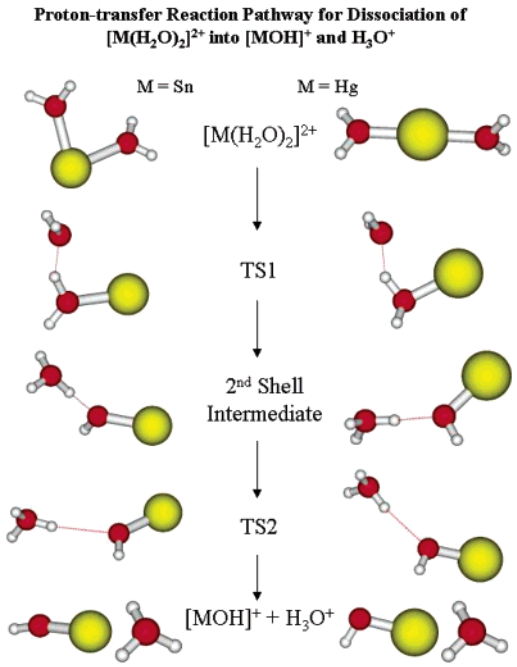

Figure 1. Calculated reaction pathways for the proton-transfer reaction $[M(H_2O)_2]^{2+} \rightarrow MOH^+ + H_3O^+$, for M = Sn^{2+} and Hg^{2+}.

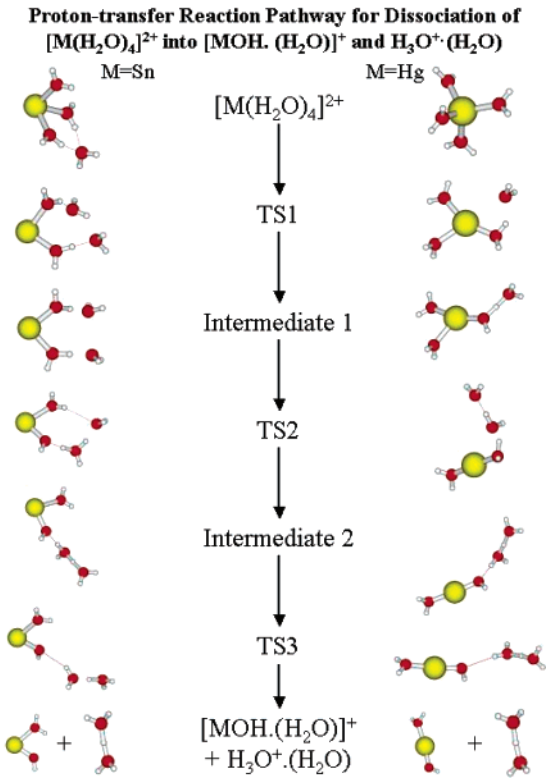

Figure 2. Calculated reaction pathways for the proton-transfer reaction $[M(H_2O)_4]^{2+} \rightarrow MOH^+(H_2O)_1 + H_3O^+(H_2O)_1$, for M = Sn^{2+} and Hg^{2+}.

gas-phase experiment. For the d^{10} Hg^{2+} ion, minimum ligand repulsion is achieved through $[Hg(H_2O)_2]^{2+}$ having a linear structure.

Both $[Sn(H_2O)_2]^{2+}$ and $[Pb(H_2O)_2]^{2+}$ are bent with oxygen−metal-oxygen bond angles of 81.8° for Sn and 84.7° for Pb. These structures are examples of the so-called "inert-pair effect"; a term that refers to the reluctance of the outer $6s^2$ electrons on Pb^{2+} (or $5s^2$ with Sn^{2+}) to be displaced or to participate in covalent bond formation.[38] It has been explained as a relativistic effect causing the 6s (or 5s) orbital to contract, thereby increasing the energy required to remove or interact with the associated electron pair.[39] In contrast, it has been shown that the d and f orbitals become destabilized because they expand radially as a result of screening by the s and p electrons due to nuclear attraction. The net result is a stable, relatively inert outer lone pair of electrons that is capable of exerting a stereochemical influence on the geometries of Sn^{2+} and Pb^{2+} complexes. Kaupp and Schleyer[40] proposed an alternative to the "inert-pair effect", which is that a difference in the radial extents of the s- and p-orbitals results in sp^n hybridization becoming increasingly unfavorable.

Either way, the lone pair of electrons can lead to a non-spherical charge distribution surrounding an M^{2+} cation (M = Sn or Pb), which results in a void in the coordination sphere that can take up more space than a single bond. The lone pair functionality in divalent lead compounds has been discussed in detail by Shimoni−Livny et al.,[38] where structures that contain an identifiable void in the coordination shell were referred to as hemi-directed. Structures with a uniform distribution of ligands were termed holo-directed.

The consequences of lone pair stereochemistry is to be seen most markedly in the structure derived for $[Sn{\cdot}(H_2O)_4]^{2+}$, which is shown in Figure 2. The most stable configuration corresponds to the metal ion having a primary coordination shell of three molecules, with the fourth molecule forming a double hydrogen bond in a secondary shell site. Previous calculations[5] involving Pb^{2+} showed the 3+1 $[Pb(H_2O)_3(H_2O)]^{2+}$ structure to be slightly more stable than the distorted tetrahedron, or butterfly configuration identified by Shimoni−Livny et al.[38] In this work, we have confirmed that the same findings apply to the tin complex, however the energy difference between the butterfly and 3+1 structure is just 8 kJ mol^{-1} (~3 kT at 298 K), which again is probably negligible in terms of the energy available in a typical gas-phase experiment, but could influence behavior in the condensed phase at room temperature. The structure shown for $[Sn{\cdot}(H_2O)_4]^{2+}$ provides a nice example of the void created by the $5s^2$ "inert" lone pair, and the 3+1 configuration subsequently proves to be an important starting configuration from which the hydrolysis reaction can be initiated. For both Ca^{2+} and Hg^{2+} the most stable $[M{\cdot}(H_2O)_4]^{2+}$ configurations were tetrahedra; however, as shown below, each ion has to move to a 3+1 arrangement before proton transfer can proceed.

(ii) M−H_2O Bond Lengths. The ionic radii of the four metal cations are given in Table 1. Since the size of a metal ion is assumed to be inversely proportional to its effective nuclear charge, a simple electrostatic (ionic) model would suggest that the M−O bond distances in $[M(H_2O)_n]^{2+}$ complexes should increase with ionic radius. Thus, the expected order for the metal ions studied here would be: Ca−O ≅ Hg−O < Sn−O < Pb−O. Assuming the Ca−O distance is approximately correct, the Hg−O bond distance is considerably shorter than expected, that of Sn−O is also too short, and only Pb−O follows the expected

(38) Shimoni-Livny, L.; Glusker, J. P.; Bock, C. W. *Inorg. Chem.* **1998**, *37*, 1853.
(39) Pyykkö, P. *Chem. Rev.* **1988**, *88*, 563.
(40) Kaupp, M.; Schleyer, P. v.R. *J. Am. Chem. Soc.* **1993**, *115*, 1061−1073.

Table 1. Comparison between Calculated Values for the Metal Ion−Oxygen Distance in $[M(H_2O)_2]^{2+}$ and $[M(H_2O)_4]^{2+}$ Complexes, and Experimental Measurements undertaken in the Condensed Phase[a]

metal	ionic radii/Å	M–O in $[M(H_2O)_2]^{2+}$/Å	M–O in $[M(H_2O)_4]^{2+}$/Å 1st shell	M–O in $[M(H_2O)_4]^{2+}$/Å 2nd shell	experimental/Å[d] 1st shell	experimental/Å[d] 2nd shell
Sn	1.22	2.29	2.34, 2.47[b]		2.33−2.34, 2.38−2.90	4.40
			2.29, 2.34[c]	4.09		
Pb[e]	1.31	2.42	2.41, 2.47[c]	4.18		
Hg	1.14	2.08	2.27		2.34−2.41	4.10
Ca	1.12	2.31	2.35		2.33	4.48−4.60

[a] From Ohtaki, H. ; Radnai, T. *Chem. Rev.* **1993**, *93*, 1157−1204. [b] Butterfly structure. [c] "3+1" structure. [d] EXAFS data. [e] NMR data only, providing evidence of 6-fold coordination.

trend. However, it will be seen below that for at least one of the metal cations a purely ionic model of bonding is not appropriate.

The structures of hydrated metal ions and their dynamical behavior in the condensed phase has been the subject of an extensive review by Ohtaki and Radnai.[41] From their compilation of EXAFS (Extended X-ray Absorption Fine Structure) data for Sn^{2+}, Hg^{2+}, and Ca^{2+} and NMR data for Pb^{2+} (EXAFS is not suitable for lead because the metal is a strong absorber of X-rays), a list of experimental metal−oxygen distances for both the first and second solvation shells has been summarized in Table 1. Calculated results from this work on $[M(H_2O)_2]^{2+}$ and $[M(H_2O)_4]^{2+}$ complexes are also given. For Ca^{2+}, it can be seen that differing degrees of coordination have a negligible effect on the metal−oxygen distance, and the calculated values are in good agreement with experiment. In contrast, the degree of coordination associated with Hg^{2+} has a profound effect on the M−O distance, with the calculations showing that a change from two to four water molecules increases the Hg−O bond length by almost 0.2 Å. Even with four molecules the calculated bond distance is still significantly shorter (∼0.15Å) than the experimental value, which is derived assuming a regular octahedral solvent structure. Furthermore, Ohtaki and Radnai[41] note that, when compared with the metal cations Cd^{2+}, Sn^{2+}, Mn^{2+} and Zn^{2+}, Hg^{2+} has the smallest second shell M−O distance, which they conclude is unusual and necessitates further investigation. Thus, for Hg^{2+}, the number of solvating ligands would appear to have an important effect on bond length and (possibly) bond strength, and the anomalously short distances observed here may merely be due to partial coordination. In the context of the study by Glusker, Bock and co-workers,[17,18,20] we note that for the metals under discussion in Table 1, there is definitely no correlation between pK_h and the calculated and/or experimental metal − oxygen bond distances. However, ΔH_h and the reciprocal of the M−O bond distance calculated for each of the $[M(H_2O)_{2,4}]^{2+}$ complexes do follow a trend.

Of particular relevance to this study are the observations of Ohtaki and Radnai on the first solvation shell of Sn^{2+}.[41] They suggest that Sn^{2+} is a peculiar ion in that it has a hydration structure that is less symmetrical than other d^{10} ions. In the six-coordinated hydration structure, two separate bond distances have been observed, one of 2.33−2.34 Å and the other 2.38−2.90 Å. Our calculations show that for $[Sn\cdot(H_2O)_4]^{2+}$ two structures are prevalent, and these differ in energy by just 8 kJ mol^{-1} (∼3 kT at 298 K). As shown in Table 1, the two structures

(41) Ohtaki, H.; Radnal, T. *Chem. Rev.* **1993**, *93*, 1157.

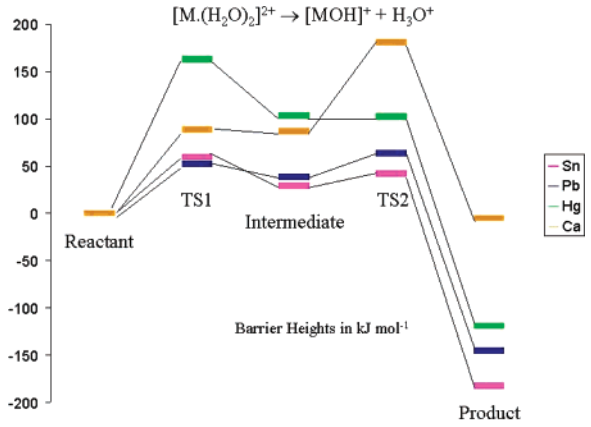

Figure 3. Energy contours for the reaction pathway $[M(H_2O)_2]^{2+} \rightarrow MOH^+ + H_3O^+$, for M = Ca^{2+}, Sn^{2+}, Pb^{2+}, and Hg^{2+}. TS1 and TS2 are transition states.

each have two long and two short bonds, and the bond lengths associated with the butterfly structure, in particular, (2.34 Å and 2.47 Å) are in excellent agreement with the range covered by the experimental data.[41] It is also pertinent to note that the calculated bond lengths for the dihydrate change very little on increasing the coordination to four, thus making comparison with the experimental six-coordinate data valid.

(iii) Reaction Intermediates. Structures corresponding to stationary points on the potential energy surface of the proton-transfer reactions for the $[Sn\cdot(H_2O)_2]^{2+}$ and $[Hg\cdot(H_2O)_2]^{2+}$ dications are shown in Figure 1; the equivalent stationary points for $[Pb\cdot(H_2O)_2]^{2+}$ is very similar to those calculated for the Tin(II) complex, and the $[Ca\cdot(H_2O)_2]^{2+}$ data are almost identical to those given by Beyer et al.[21] The relative energies of $[Sn\cdot(H_2O)_2]^{2+}$, $[Pb\cdot(H_2O)_2]^{2+}$, and $[Hg\cdot(H_2O)_2]^{2+}$ along the reaction coordinate are shown in Figure 3, where a comparison is made with the calculated data for $[Ca\cdot(H_2O)_2]^{2+}$. Tables 2 and 3 respectively, provide a summary of important geometric parameters and the results of a natural population analysis associated with each of the structures identified in Figure 1. In presenting these data we follow the format adopted by Beyer et al.[21] and label key positions along the reaction profile as being either transition states or intermediates; the distinction between the two being respectively the presence or absence of a reaction coordinate in the form of a single imaginary frequency. The first step in the reaction sequence involves promoting one water molecule to the second solvation shell via transition state 1 (TS1). Qualitatively, all four ions adopt a similar geometry for TS1, although as Table 2 shows, there are significant variations in several of the inter- and intramolecular bond lengths. The first important difference between the metal cations comes with formation of the 2nd shell intermediate. As seen from Figure 1, for the acidic cations, this structure is already displaying evidence of proton transfer. In contrast, $[Ca\cdot(H_2O)_2]^{2+}$ follows the pattern seen by Beyer et al.[21] and adopts a structure that is essentially a second solvation shell. Further evidence of geometric differences between the ions is to be seen in Table 2c, where O−H bond distances for the second shell structures of Sn^{2+}, Pb^{2+}, and Hg^{2+} are quite different from those of Ca^{2+}. For the latter ion, proton transfer to form H_3O^+ occurs after the intermediate but prior to transition state 2 (TS2), which is again in agreement with the results of Beyer et al.[21]

Table 2. Geometric Parameters for the Stationary Points of the Reaction $[M(H_2O)_2]^{2+} \rightarrow [MOH]^+ + H_3O^+$[a]

A. M–O1 distance (Å)

M	$M^{2+}(H_2O)_2$	TS1	second shell	TS2	$MOH^+ + H_3O^+$
Sn	2.29	2.08	2.05	1.99	1.89
Pb	2.42	2.27	2.18	2.10	2.00
Hg	2.08	2.09	2.04	2.03	2.01
Ca	2.31	2.20	2.19	2.01	1.93

B. M–O2 distance (Å)

M	$M^{2+}(H_2O)_2$	TS1	second shell	TS2	$MOH^+ + H_3O^+$
Sn	2.29	3.11	4.28	5.22	∞
Pb	2.42	3.49	4.31	5.53	∞
Hg	2.08	3.01	4.44	5.01	∞
Ca	2.31	3.70	4.11	5.83	∞

C. O1–H1 distance (Å)

M	$M^{2+}(H_2O)_2$	TS1	second shell	TS2	$MOH^+ + H_3O^+$
Sn	0.98	1.05	1.53	2.56	∞
Pb	0.98	1.02	1.39	2.73	∞
Hg	0.98	1.04	1.72	2.28	∞
Ca	0.98	1.02	1.04	3.09	∞

D. O2–H1 distance (Å)

M	$M^{2+}(H_2O)_2$	TS1	second shell	TS2	$MOH^+ + H_3O^+$
Sn	3.11	1.50	1.04	0.98	0.97
Pb	3.36	1.55	1.08	0.98	0.97
Hg	4.77	1.54	1.00	0.98	0.99
Ca	5.28	1.57	1.46	0.98	0.96

[a] The distances are defined in the text.

Table 3. Natural Partial Charges for the Stationary Points of the Reaction $[M(H_2O)_2]^{2+} \rightarrow MOH^+ + H_3O^+$

metal	location[a]	M^{2+}	O (MOH^+)	O (H_3O^+)	H (MOH^+)
Ca	start	1.96	−1.14	−1.14	0.58
	TS1	1.97	−1.20	−1.04	0.58
	intermediate	1.97	−1.22	−1.02	0.57
	TS2	1.91	−1.43	−0.85	0.52
	product	1.88	−1.42	−0.85	0.54
	total charge transfer = 0.4e				
Sn	start	1.86	−1.12	−1.12	0.6
	TS1	1.89	−1.20	−1.04	0.61
	intermediate	1.83	−1.31	−0.89	0.57
	TS2	1.77	−1.32	−0.86	0.55
	product	1.71	−1.30	−0.85	0.59
	total charge transfer = 0.34e				
Pb	start	1.88	−1.11	−1.11	0.59
	TS1	1.90	−1.17	−1.04	0.60
	intermediate	1.85	−1.27	−0.91	0.56
	TS2	1.76	−1.29	−0.85	0.54
	product	1.69	−1.25	−0.85	0.57
	total charge transfer = 0.36e				
Hg	start	1.67	−1.06	−1.06	0.62
	TS1	1.77	−1.06	−1.06	0.61
	intermediate	1.60	−1.11	−0.87	0.55
	TS2	1.53	−1.06	−0.85	0.53
	product	1.36	−0.88	−0.85	0.52
	total charge transfer = 0.23e				

[a] With respect to the stationary points identified on the reaction pathway given in Figure 1.

In all cases, TS2 arises as the result of coulomb repulsion between the separating positive charges. In effect, it is the point at which the steep wall of the repulsive charge-transfer potential surface makes an avoided crossing with the attractive surface that exists between the metal dication and individual water molecules. The late onset of proton transfer on the part of Ca^{2+} is probably responsible for the high coulomb barrier seen for TS2 in Figure 3 (see below).

The second shell intermediates seen for Sn^{2+}, Pb^{2+}, and Hg^{2+} take the form of salt bridges that are stabilized by the attraction between OH^- and H_3O^+. In the case of Sn^{2+} and Pb^{2+}, this interaction is sufficiently strong as to give intermediate structures that are stable with respect to both the reverse and forward reaction pathways. For Hg^{2+} the potential energy profile would suggest a transitory proton transfer state that is on a gradual downhill trajectory, and for Ca^{2+} anything resembling a salt bridge only occurs as the complex approaches TS2. Apart from Ca^{2+}, the sequence of events involving Sn^{2+}, Pb^{2+} and Hg^{2+} is slightly different from that proposed by Beyer et al.,[21] because the latter discussed proton transfer in terms of a "salt bridge mechanism" rather that in terms of identifiable intermediates. However, since the overall reaction mechanism will conserve total energy (potential + kinetic), what are identified as stable (potential energy) intermediates will in fact be transients as far as the reactions are concerned.

The MOH^+ product shows distinct differences across the four metals, both in terms of structure and charge distribution. As might be expected for calcium, $CaOH^+$ is linear. In contrast, the other three MOH^+ products are all bent: in $SnOH^+$ the bond angle is 167°; $PbOH^+$, 144°; and $HgOH^+$, 107°. For tin and lead, the bent geometry is again as a consequence of the s^2 lone pair on the metal ion. However, in the case of mercury, where there are no such effects, the comparatively small bond angle is as a result of increased charge transfer predominantly between the metal ion and the oxygen atom in $HgOH^+$ (see Table 3).[16] The change in geometry results in a better alignment between the empty sdσ hybrid orbital on Hg^{2+} and the energetically labile lone electron pair located on the in-plane p orbital of oxygen.

Changes in the M−O bond length during the course of the hydrolysis process also reveal interesting patterns of behaviour that appear to be strongly influenced by charge distribution (see Table 3). Thus, the short Hg−O bond is not too unexpected when the appropriate natural charge populations are analyzed. Furthermore, on going from the reactant ion to the hydrolysis product, the Hg−O1 bond-distance changes by just 0.07 Å, which shows that the character of the bond alters very little as a result of reactivity. In contrast, the other metals each show a considerable reduction in M−O1 bond distance (∼0.4 Å) on going from the reactant complex to the charge-transfer product. Even the final step in the reaction sequence, removal of the polarizing H_3O^+, results in relaxation to an even shorter M−O1 distance in the free MOH^+ ion. It is also interesting to note that there is very little change in the Hg−O−H^+ bond angle on going from reactant ion to hydrolysis product.

The M−O2 bond distance (Table 2b) increases rapidly as one water molecule is promoted from the first to the second solvation shell, and then finally as the separation of H_3O^+ occurs via Coulomb repulsion. However, in the transition state for this final step it can be seen that for the two most acidic metal cations, Hg^{2+} and Sn^{2+}, the M−O2 distances are much shorter that those calculated for Pb^{2+} and Ca^{2+}. This observation would imply that enhanced reactivity may be associated with charge transfer occurring early in the reaction coordinate. Support for this suggestion is to be seen in the O1−H1 and O2−H1 data presented in Table 3, parts c and d, respectively. Likewise, the data presented by Beyer et al.[21] on $Be^{2+}(H_2O)_2$ is an extreme example of this behavior; however, in these circumstances, the small size of the Be^{2+} cation also has a significant influence on the outcome. What is clear from the data presented here is that the sequence of events in these dihydrates is much less

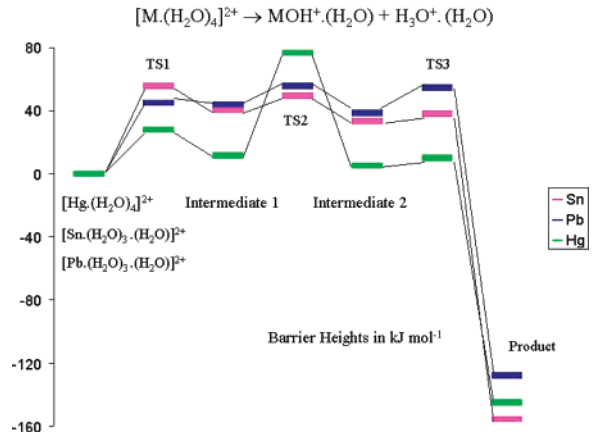

Figure 4. Energy contours for the reaction pathway $[M(H_2O)_4]^{2+} \rightarrow MOH^+(H_2O)_1 + H_3O^+(H_2O)_1$, for M = Sn^{2+}, Pb^{2+} and Hg^{2+}. TS1, TS2, and TS3 are transition states.

Table 4. Natural Partial Charges on the Metal Cations for the Stationary Points of the $[M(H_2O)_4]^{2+}$ Proton Transfer Reaction Pathway

	Ca^{2+}	Sn^{2+}	Pb^{2+}	Hg^{2+}
start	1.907	1.769	1.798	1.722
TS1	not observed	1.804	1.810	1.666
Int 1	1.932	1.780	1.804	1.626
TS2	1.897	1.759	1.774	1.602
Int2		1.742	1.755	1.489
TS3		1.697	1.692	1.435
product	1.885	1.651	1.644	1.372

dependent on the ionic radius of the cation than was observed by Beyer et al.[21] in their calculations on the alkaline earth metals.

In the case of the $[M(H_2O)_4]^{2+}$ complexes, it can be seen from a cartoon of the reaction profiles for $[Sn\cdot(H_2O)_4]^{2+}$ and $[Hg\cdot(H_2O)_4]^{2+}$ (Figure 2) that the sequence of events leading to proton transfer is more complex than that seen for $[M\cdot(H_2O)_2]^{2+}$ dications. Each reaction sequence is clearly too complicated to warrant the type of detailed breakdown presented for the dihydrates. However, to help in the analysis of these data, Figure 4 presents a summary of the relative energies of each of the stationary points along the reaction pathway, and Table 4 gives the results of a natural population analysis on all of the metal ions. $[Sn\cdot(H_2O)_4]^{2+}$ and $[Pb\cdot(H_2O)_4]^{2+}$ follow reaction paths that are very similar. However, in contrast to the other dications, the pathway for $[Ca(H_2O)_4]^{2+}$ is very straightforward, with a single water molecule being promoted to the second shell and proton transfer leading to the products $CaOH^+\cdot(H_2O)_2 + H_3O^+$; a sequence of events that is not too different from the steps shown in Figure 3. However, while all the other $[M(H_2O)_4]^{2+}$ complexes favor the loss of $H_3O^+\cdot H_2O$, the only pathway found for Ca^{2+} resulted in the loss of H_3O^+.

For both $[Sn(H_2O)_4]^{2+}$ and $[Pb(H_2O)_4]^{2+}$ the starting structures are quite different from those given in Figure 1, and even through the complexes already have one water molecule occupying a second shell site, the first step in the proton transfer sequence requires the promotion of a second molecule. As Figure 4 shows, this step has a modest reaction barrier associated with it, and the reason can be seen in Table 4 where the charge on the metal ion is calculated to increase slightly with the removal of a first-shell water molecule. For both complexes the reaction pathway proceeds through the formation of a quasi-cyclic hydrogen bonded structure within which proton transfer occurs. The reaction sequence is completed when the cyclic structure opens and $H_3O^+H_2O$ is lost. Finally, for $[Hg(H_2O)_4]^{2+}$ two water molecules are promoted sequentially from the primary shell, but no cyclic arrangement is observed, and when compared with Sn and Pb, the final proton-transfer step occurs a little later in the reaction sequence.

There are several qualitative observation to be made when comparing the $[M(H_2O)_4]^{2+}$ complexes for differences in behavior. For Sn^{2+}, Pb^2, and Hg^{2+} it is clearly energetically more favorable to promote two water molecules and lose $H_3O^+H_2O$, rather than follow the route adopted by Ca^{2+}, which is to move one molecule and lose H_3O^+. Formation of the quasi-cyclic intermediates and transition states by Sn^{2+} and Pb^{2+} are probably further evidence of stereochemical influence by the s^2 electrons; however, these cyclic structures do also appear to facilitate proton transfer. In contrast, the more open structures seen for $[Hg(H_2O)_4]^{2+}$ and the reaction intermediates, do require more energy to move the second water into a position that aids proton transfer (see Figure 4). As before, there are structures that can be equated with the formation of a salt bridge; thus, both Sn^{2+} and Pb^{2+} have stable intermediates that correspond to $H_3O^+\cdot H_2O$ attracted to OH^- and this time Hg^{2+} also falls into that group. In contrast, Ca^{2+} follows a pattern similar to that seen for $[Ca(H_2O)_2]^{2+}$ where proton transfer occurs at the final transition state.

The contrast between Ca^{2+} and the other metal cations in terms of the number of water molecules lost during proton-transfer warrants further discussion. A search for the reaction pathway: $[Sn(H_2O)_4]^{2+} \rightarrow SnOH^+(H_2O)_2 + H_3O^+$, revealed an energy profile very similar in shape to that calculated for $[Ca(H_2O)_2]^{2+}$ (Figure 3), but with the final barrier and the exothermicity shifted down by approximately 100 kJ mol^{-1}. The significant features are a high ($\sim$90 kJ mol^{-1}) barrier to reach TS2, and a final exothermicity that is $\sim$50 kJ mol^{-1} less than that calculated for the pathway that involves the loss of $H_3O^+H_2O$. Very similar behavior on the part of $[Pb(H_2O)_4]^{2+}$ is to be seen in ref 5 (Figure 3), where there is a substantial difference in exothermicity between reaction pathways involving the loss of $H_3O^+H_2O$ and H_3O^+.

Recent calculations by Beyer and Metz[42] show that for hydrated Co^{2+} the proton-transfer step is $[Co(H_2O)_4]^{2+} \rightarrow CoOH^+(H_2O)_2 + H_3O^+$, which supports observations from an experimental study of the reaction by Metz and co-workers.[43] However, there are also numerous examples of reactions induced in size-selected $[M(H_2O)_4]^{2+}$ ions where $MOH^+(H_2O)$ and $H_3O^+H_2O$ feature prominently as the proton-transfer products.[3,7,8] Given these observations and the fact that the ions Sn^{2+}, Pb^{2+}, and Hg^{2+} are inherently unstable in the presence of small numbers of water molecules, leads us to believe that reaction pathways which are slightly different from those determined in other calculations are to be expected.

(iv) Natural Population Analysis. Charges calculated from a natural charge population analyses using the MP2 density are given in Table 3 for atoms involved in stationary points along the reaction pathways of all $[M(H_2O)_2]^{2+}$ complexes. Table 4 presents similar data for $[M(H_2O)_4]^{2+}$, but only for the metal ions. Some of these results have already been discussed in conjunction with an analysis of the reaction pathways; however,

(42) Beyer, M. K.; Metz, R. B. *J. Phys. Chem. A* **2003**, *107*, 1760.
(43) Faherty, K. P.; Thompson, C. J.; Aguirre, F.; Michne, J.; Metz, R. B. *J. Phys. Chem. A* **2001**, *105*, 10 054.

this section presents a brief overview of the results. In all cases, the charges on the hydrogen atoms (both participants and spectators) do not change significantly; such behavior is consistent with only the oxygen atoms undergoing a change in formal charge within the Lewis formalism (partial donation of an electron pair). Similarly, more electron density is transferred to the metal cation from the hydroxide moiety than from any of the water molecules, but the extent of charge transfer differs greatly between four metal cations. For Ca^{2+}, most transfer of charge during the reaction occurs between oxygen atoms ($OH^- \leftarrow H_3O^+$), with negligible involvement on the part of the metal ion. In agreement with previous work on Ca^{2+},[21] the most significant change in charge density occurs at TS2 during proton transfer.

For both Sn and Pb, the charge gained from H_3O^+ by the MOH^+ moiety is shared almost equally between the metal and the oxygen. A small amount (0.03e), moves before the intermediate structure is reached, but the majority of charge is transferred as the system moves through TS2. In contrast, Hg is sufficiently electrophillic that it is actually reduced by the oxygen atom in the MOH^+ fragment (i.e., the charge on the oxygen is lower than that seen in $[Hg(H_2O)_2]^{2+}$). As with Sn and Pb, a small amount of charge (0.06e) is transferred during the displacement of a water molecule; but the majority (0.24e) is transferred during the separation of $[HgOH]^+$ and H_3O^+. Although geometric factors appear to promote greater participation of the metal ion in the case of Sn and Pb, the rearrangement of charge is qualitatively similar to that seen for Ca, i.e., the charge on the oxygen atom of the MOH^+ fragment increases at the expense of the H_3O^+ fragment, showing the Lewis acid view of events to be qualitatively correct.

In contrast to the predominantly ionic behavior of Ca^{2+} and, to a lesser degree, Sn and Pb all bond formation processes involving Hg^{2+} display significant covalent character from the onset of complex formation. In $[Hg(H_2O)_2]^{2+}$ the charge on the mercury atom is +1.67e, and the difference between this and the formal charge of +2 is gained primarily at the expense of the coordinating oxygen atoms. The Hg cation continues to gain electron density as it moves along the reaction pathway, culminating in $HgOH^+$ having gained over 0.3e, which is to be compared with Ca, where the gain is just 0.02e. Furthermore, it should be noted that the charge on the oxygen in $[HgOH]^+$ is approximately equal to that on the oxygen atom in H_3O^+; thus it might be more appropriate to consider $[HgOH]^+$ as $[M^+-OH^\bullet]$ rather than $[M^{2+}-OH^-]$.

In comparing the data in Table 3 for the dihydrates with the natural charges given in Table 4 for the $[M(H_2O)_4]^{2+}$ complexes there are several notable differences. Ca, Sn, and Pb all show a reduction in charge due presumably, to increased stabilization by the presence of more water molecules. In contrast, the positive charge on mercury increases in magnitude with the addition of further water molecules. Likewise, the MOH^+ products all show the same trend, although $CaOH^+$ remains strongly ionic despite additional solvation. With regard to the overall acidity of the cations, it is interesting to note that the magnitude of the charge difference on Hg before and after hydrolysis increases with solvation, whereas the other three metal cations all show a slight decrease.

(v) Energetics. The various reaction barriers associated with the hydrolysis process in $[M(H_2O)_2]^{2+}$ and $[M(H_2O)_4]^{2+}$ complexes are shown in Figures 3 and 4, respectively. There are two obvious sources of barrier—(i) displacement of a water molecule(s) from the primary solvation shell, and (ii) proton transfer or curve crossing. If Figures 3 and 4 are examined in conjunction with the schematics of the reaction profiles (Figures 1 and 2) then it is possible to match the energy barriers with steps in the hydrolysis mechanism. Thus, for $[Hg(H_2O)_2]^{2+}$ the highest point in the reaction profile occurs as a result of displacement of a water molecule from the primary shell. The comparatively high energy required to execute this step may be as a consequence of the covalent character of the metal−oxygen bond. In contrast, the most significant barrier for the $[Ca(H_2O)_2]^{2+}$ system corresponds to the point of proton transfer. Both $[Sn(H_2O)_2]^{2+}$ and $[Pb(H_2O)_2]^{2+}$ offer comparatively little resistance to movement along the reaction coordinate.

Table 5. Gibbs Free Energies for the Reactions $[M(H_2O)_2]^{2+} \rightarrow [MOH]^+ + H_3O^+$ and $[M(H_2O)_4]^{2+} \rightarrow [MOH{\cdot}H_2O]^+ + H_3O^+{\cdot}H_2O$ at 298.15 K and 1 Atm

	ΔG/kJ mol^{-1}		ΔG/kJ mol^{-1}
$[Sn(H_2O)_2]^{2+}$	−220.1	$[Sn(H_2O)_4]^{2+}$	−220.6
		$[Sn(H_2O)_3{\cdot}H_2O]^{2+}$	−198.1
$[Pb(H_2O)_2]^{2+}$	−176.8	$[Pb(H_2O)_3{\cdot}H_2O]^{2+}$	−168.5
$[Hg(H_2O)_2]^{2+}$	−151.3	$[Hg(H_2O)_4]^{2+}$	−181.8
$[Ca(H_2O)_2]^{2+}$	−37.6	$[Ca(H_2O)_4]^{2+}$	+19.8

For the $[M(H_2O)_4]^{2+}$ complexes, it can be seen that in the case of four-coordinate Hg^{2+}, the barrier to water displacement has dropped significantly when compared with $[Hg(H_2O)_2]^{2+}$; possibly due to a combination of steric interactions and a reduced level of covalent bonding. The most pronounced barrier on the $[Hg(H_2O)_4]^{2+}$ profile now occurs at the point of proton transfer; however, the magnitude is only slightly smaller than that seen for $[Hg(H_2O)_2]^{2+}$. Interestingly, both $[Sn(H_2O)_4]^{2+}$ and $[Pb(H_2O)_4]^{2+}$ again offer little resistance to movement along the reaction coordinate, and the potential energies required are almost no different from those calculated for the dihydrates.

Although the energy barriers discussed above will have very significant effects on events taking place in the gas phase, an understanding of the energetics of acidity in the bulk only requires knowledge of changes in Gibbs free energy.[24] This quantity has been calculated for each of the metal cations undergoing hydrolysis in the presence of two and four water molecules and the results are shown in Table 5. As might be expected from the data given in Figures 3 and 4, most of the values for ΔG are large and negative. However, there are interesting trends. First, the two most acidic metal cations, Sn^{2+} and Hg^{2+}, have free energies that remain large and negative as the number of water molecules is increased. Second, the energy change for Pb^{2+} shows some decline as the number of waters is increased, but the value still remains large and negative. Finally, for the least acidic cation, Ca^{2+}, the Gibbs free energy change becomes increasingly more positive as the degree of solvation increases. This latter observation is consistent with data presented by Glusker, Bock and co-workers on the behavior of a range of dications as a function of increasing levels of solvation.[17,18] For the solvation of Ca^{2+} to match the experimental value of pK_h, ΔG would have to increase to ~+30 kJ mol^{-1}. The order of negative change in Gibbs free energy calculated for the $[M(H_2O)_4]^{2+}$ complexes is $Sn^{2+} > Hg^{2+} > Pb^{2+} > Ca^{2+}$ which is precisely the same order as their acidities.

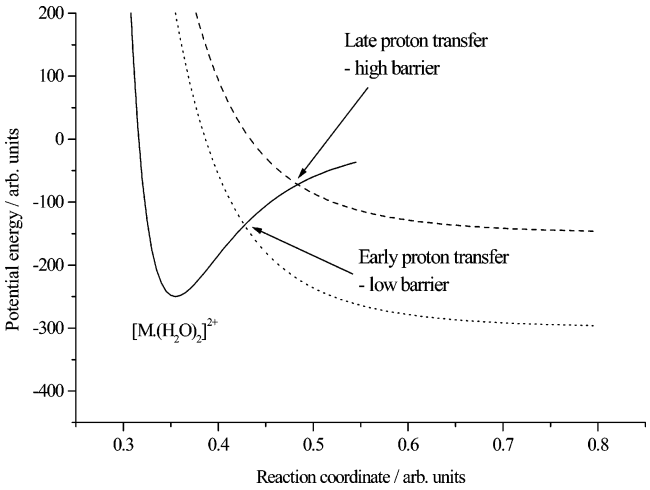

Figure 5. Schematic representation of influence early proton transfer has on barrier height.

4. Conclusion

If Ca^{2+} is taken as a reference point, then there are obvious features associated with the behavior of the other three metal cations, Sn^{2+}, Pb^{2+}, and Hg^{2+}, that distinguishes them as being more acidic. Examining behavior that would be relevant to ions in the gas-phase first, it can be seen from the results that for Sn^{2+}, Pb^{2+}, and Hg^{2+}, successive solvation lowers the barrier to hydrolysis and that once water molecules have moved into the appropriate sites there are no further energy constraints to hydrolysis. Given the level of internal energy these ions might acquire when generated, the calculated barriers to water displacement are not particularly significant. Schematically, the sequence of events leading to hydrolysis can be summarized as shown in Figure 5, where proton transfer is depicted purely in terms of a (avoided) curve crossing process: a low barrier accompanies early proton transfer and as the barrier increases in magnitude so the point of proton transfer is shifted further along the reaction coordinate. Figure 3 portrays this pattern of behaviour quite precisely on the part of $[M{\cdot}(H_2O)_2]^{2+}$ complexes, and in the case of $[Sn{\cdot}(H_2O)_4]^{2+}$, a high, late barrier is also observed when the reaction pathway involves the loss of H_3O^+ rather than $H_3O^+H_2O$. Such behavior could be associated with the charge on H_3O^+ being in close proximity to the hydrogen bond that is finally broken to release the two fragment ions. This arrangement would polarize the electron density on the adjacent oxygen atom, which in turn would increase the strength of the hydrogen bond.

With regard to possible future experiments, the point of curve crossing might also be expected to influence energy partitioning: early proton transfer might lead to a comparatively modest release of kinetic energy, influenced by the combination of a low barrier and the formation of a quasi-stable intermediate bound by the attraction between OH^- and H_3O^+. In contrast, late proton transfer gives no such intermediate, but may lead to enhanced kinetic energy release due to partitioning of a larger repulsive barrier in the exit channel.

When comparing Hg^{2+} and Pb^{2+} (or Sn^{2+}) we can note that although the barrier − proton transfer relationship may influence events in the gas phase, the important factor in the condensed phase is the free energy difference between either side of the equilibrium given by eq 1. From the calculations, it can be seen that for both Pb^{2+} and Sn^{2+} the inert lone pair has an effect on ligand geometry. In the condensed phase, this anisotropy is clearly evident both in terms of the structures adopted by Pb^{2+} complexes and in the spatial distribution of water molecules surround Sn^{2+} in solution.[41] In aqueous solution, a consequence of the stereochemical influence of the inert lone pair will be for the high electron density on one side of either Sn^{2+} or Pb^{2+} to force donor molecules into positions that facilitate proton transfer. In addition, as part of the normal random behavior of bulk water, acceptor molecules will constantly be moving in and out of sites suitable for proton transfer. In effect, the normal behavior of molecules in bulk water will eliminate any barriers that involve the displacement of water, leaving only that associated with a break up of the salt bridge structure. This behavior on the part of Sn^{2+} and Pb^{2+} will lead to early proton transfer and the overall effect will be a low value for ΔG and hence a comparatively high acidity.

For Hg^{2+} circumstances surrounding the acidity of the ion are slightly different from those for Sn^{2+} and Pb^{2+}. An examination of Figures 3 and 4 shows that the only significant energy barriers along the reaction pathway for Hg^{2+} hydrolysis involve the movement of water molecules. As already discussed, these processes are not going to be important in solution because the ion will always have water molecules constantly moving in and out of sites favorable for proton transfer. What appears to facilitate hydrolysis on the part of Hg^{2+} are the observations that: (i) the reaction for this cation involves the minimum amount of charge transfer (see Table 3); and (ii) there is negligible change (−0.07 Å) in the Hg−O bond distance during the course of the reaction. Both these factors are intimately associated with the high degree of covalent character exhibited by bonds involving both Hg^{2+} and Hg^+. In solution, the process of hydrolysis will be further assisted by the exothermic step[1]

$$HgOH^+ + OH^- \Leftrightarrow Hg(OH)_2\,(aq) \qquad (4)$$

When compared with Ca^{2+}, which has a comparable ionic radius, Hg^{2+} is able to polarize electron density away from the coordinating water molecules. Such behavior makes a significant contribution to the covalency of Hg^{2+} complexes, and reduces the degree of electron rearrangement required during proton transfer.

In summary, the three metal ions, Sn^{2+}, Pb^{2+}, and Hg^{2+} would appear to be anomalously acidic in the gas phase because the most significant barriers to proton-transfer involve the displacement of water molecules. In solution the thermal motion of individual water molecules would minimize such barriers. This behavior contrasts with that of our reference cation, Ca^{2+}, for which it is found that movement of the proton contributes to a high reaction barrier. The calculated values of ΔG for Sn^{2+}, Pb^{2+}, and Hg^{2+} all favor spontaneous proton transfer, which again contrast with results obtained for Ca^{2+} where ΔG becomes progressively more positive as the degree of solvation increases.

Acknowledgment. The authors would like to thank EPSRC for financial support and for the award of an Advanced Research Fellowship to H.C. All calculations were performed on an ONYX 2 belonging to the Sussex High Performance Computing Initiative.

JA039248P